

Parametric Surface Modeling and Registration for Comparison of Manual and Automated Segmentation of the Hippocampus

Li Shen, Hiram A. Firpi, Andrew J. Saykin, and John D. West

IU Center for Neuroimaging, Imaging Sciences Division, Department of Radiology
Center for Computational Biology and Bioinformatics
Indiana University School of Medicine
950 W Walnut St, R2 E124, Indianapolis, IN 46202
{shenli,hfirpi,asaykin,jdwest}@iupui.edu

Abstract. Accurate and efficient segmentation of the hippocampus from brain images is a challenging issue. Although experienced anatomic tracers can be reliable, manual segmentation is a time consuming process and may not be feasible for large-scale neuroimaging studies. In this paper, we compare an automated method, FreeSurfer (V4), with a published manual protocol on the determination of hippocampal boundaries from MRI scans, using data from an existing MCI/AD cohort. To perform the comparison, we develop an enhanced spherical harmonic processing framework to model and register these hippocampal traces. The framework treats the two hippocampi as a single geometric configuration and extracts the positional, orientation and shape variables in a multi-object setting. We apply this framework to register manual tracing and FreeSurfer results together and the two methods show stronger agreement on position and orientation than shape measures. Work is in progress to examine a refined FreeSurfer segmentation strategy and an improved agreement on shape features is expected.

Key words: Shape analysis, segmentation, registration, hippocampus

1 Introduction

The hippocampus has been extensively studied with neuroimaging techniques given its importance in learning and memory and its potential as a biomarker for brain disorders such as Alzheimer’s disease [1–4], epilepsy [5] and schizophrenia [6–8]. While some groups used automated methods for quantification of the size and shape of the hippocampus [3–6, 9], in most studies [1, 2, 7, 8, 10, 11], hippocampal segmentation from magnetic resonance imaging (MRI) scans was done manually by anatomic tracers using software tools that were either in-home made or publicly available (e.g., Brains [12], 3D Slicer [13], ITK-SNAP [14]). Many of these tools provide not only manual tracing capabilities but also semi-automatic approaches involving less human interaction.

Accurate and efficient segmentation of the hippocampus from brain images is still a challenging issue. Although experienced anatomic tracers can be reliable, manual segmentation is a time consuming process and may not be feasible for large-scale neuroimaging studies. For example, the Alzheimer’s Disease Neuroimaging Initiative (ADNI) [15] collects 1.5T structural MRI for over 800 subjects every 6 or 12 months for 2-3 years. Manual segmentation is apparently not an ideal method for handling such a study involving thousands of MRI scans.

A feasible strategy for hippocampal segmentation in large-scale studies should be able to minimize human intervention in the processing pipeline. Diffeomorphic mapping is a notable method for automatic segmentation and has been used by Csernansky and colleagues in many hippocampal studies [3–6]. FreeSurfer [16–18] is an automatic software tool for whole brain segmentation and cortical parcellation. Due to its open source license, FreeSurfer has been widely used in the neuroimaging field. Two recent studies reported similar results on comparing hippocampal volumes measured using their own manual method and a specific version of FreeSurfer (V4 in [19], V3.04 in [20]): the intraclass correlation coefficients (ICCs) were both between 0.8 and 0.85, showing good agreement.

In this paper, we extend our previous work [19] to compare hippocampal morphometric features beyond the volume. We develop an enhanced spherical harmonic (SPHARM) processing framework to model and register the hippocampal traces. The framework treats the two hippocampi as a single configuration and extracts the positional, orientation and shape variables in a multi-object setting. The proposed registration algorithm operates directly on the SPHARM coefficients and thus is not only effective but also efficient. We apply this framework to register all the hippocampal data together and to decouple the position, orientation, and shape for comparing the manual and FreeSurfer results. The proposed shape modeling and registration framework can also be used as a general purpose tool for other shape comparison and analysis applications.

2 Hippocampal Data

In this work, we use a data cohort for studying memory circuitry in mild cognitive impairment (MCI) and early Alzheimer’s disease (AD). In this MCI/AD cohort, there are hippocampal data available for 123 subjects total, in four categories: 39 healthy older adults (HC), 38 euthymic older adults with cognitive complaints (CC) but intact neuropsychological performance, 36 older adults with amnesic MCI, and 10 adults with AD. Volumetric structural MRI data were acquired on a 1.5 Tesla GE LX Horizon scanner using a T1-weighted SPGR coronal series with 1.5mm slice thickness. Further details about this data set are available in [2]. Hippocampal and intracranial boundaries were obtained using (1) a manual protocol reported in [10] using the BRAINS software package [12], and (2) a fully automated method using the FreeSurfer V4 package [16–18].

For manual segmentation, images were reformatted into isotropic 1-mm voxels and resampled into the plane perpendicular to the long axis of the hippocampus using BRAINS [12]. Manual traces were performed in the coronal plane using

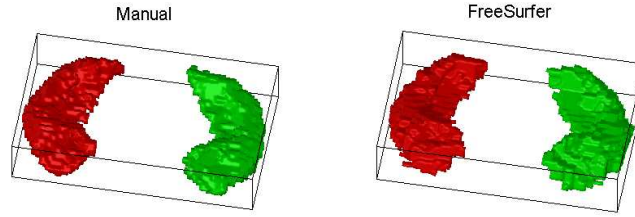


Fig. 1. Sample segmentation results generated by manual tracing (left) and FreeSurfer (right): Each hippocampus is described by a binary image and the corresponding voxel surface is displayed. Left hippocampi are shown in green and right in red.

markings placed in the axial and sagittal views to guide boundary determination. A 3D binary image was reconstructed from each set of 2D traces. Further details about this manual protocol is available in [10]. For automated segmentation, FreeSurfer was employed to automatically label subcortical tissue classes using an atlas-based Bayesian segmentation procedure (see [18] for further details). We ran the complete FreeSurfer pipeline without any manual intervention on an IBM HS21 Bladeserver cluster running Red Hat Linux. Each slice of segmentation label map was inspected by a technician and passed a basic test of quality control. From each label map, we extracted the left and right hippocampi as two 3D binary images. Fig. 1 shows sample manual and FreeSurfer results. For convenience, in the rest of the paper, we use **MT** to indicate the manual tracing method and **FS** to indicate the FreeSurfer method.

3 Surface Modeling and Registration

We recently compared hippocampal volume determined by the MT and FS methods and they showed good agreement (ICCs ranging from 0.8 to 0.85) [19]. Since regional differences in shape are more likely to reveal clues to pathophysiology than volume, it is critical to examine differences in extracted shape features using various methods. This paper is focused on examining these morphometric features. We employ the spherical harmonic (SPHARM) description [21] to model the hippocampal surfaces and develop an enhanced SPHARM registration algorithm to facilitate the comparison between the MT and FS data. This method is designed for comparing segmentation methods performed in two different image spaces (e.g., in our MT and FS cases) without knowing their spatial relationship. If this relationship is known, these two spaces can be easily registered together and direct 3D volume comparison as proposed in [18] can be applied.

SPHARM [21] is a highly promising surface modeling method to model arbitrarily shaped but simply connected 3D objects, and has been successfully applied to numerous applications in brain imaging (e.g., [22, 23]). SPHARM is used in this study for modeling all the hippocampal surfaces. Its first step is to create a continuous and uniform mapping from the object surface to the surface of a

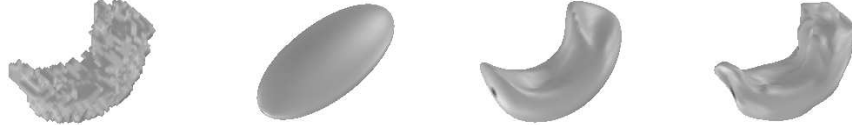


Fig. 2. Sample SPHARM reconstructions: Shown from left to right are original surface and SPHARM reconstructions up to degrees 1, 5 and 15.

unit sphere. The result is a bijective mapping between each point \mathbf{v} on a surface and a pair of spherical coordinates θ and ϕ : $\mathbf{v}(\theta, \phi) = (x(\theta, \phi), y(\theta, \phi), z(\theta, \phi))^T$.

The object surface can then be expanded into a complete set of spherical harmonic basis functions Y_l^m , where Y_l^m denotes the spherical harmonic of degree l and order m . The expansion takes the form: $\mathbf{v}(\theta, \phi) = \sum_{l=0}^{\infty} \sum_{m=-l}^l \mathbf{c}_l^m Y_l^m(\theta, \phi)$, where $\mathbf{c}_l^m = (c_{xl}^m, c_{yl}^m, c_{zl}^m)^T$. The coefficients \mathbf{c}_l^m can be estimated up to a user-desired degree by solving a set of linear equations in a least squares fashion. The object surface can be reconstructed using these coefficients, and using more coefficients leads to a more detailed reconstruction (Fig. 2). The degree one reconstruction is always an ellipsoid. We call it the *first order ellipsoid* (FOE).

Surface registration aims to register all the models into a common reference system to facilitate shape comparison. It creates a normalized geometric representation to describe the shape after normalizing the size, position and orientation measures (i.e., excluding scaling, translation, and rotation). Since the relative position and orientation between the two hippocampi (or the pose of the hippocampal pair) are of our interest, we treat the two hippocampi as a single configuration and study SPHARM registration in a multi-object setting.

Scaling invariance can be achieved by multiplying the coefficients by a scaling factor to normalize a certain volume. We normalize the intracranial volume (ICV) to account for the brain size variation: (1) the mean ICV ($= 1421.2 \text{ cm}^3$) of the MT data is calculated, and (2) each hippocampal pair in both MT and FS data is scaled proportionally along with the corresponding ICV so that the ICV is normalized to 1421.2 cm^3 .

While ignoring the degree 0 coefficient results in translation invariance for a single SPHARM model, in our multi-object setting, new methods need to be developed to preserve the relative position among objects while removing the global translation effect. The surface registration methods described below aim to remove the effects of both global *translation* and global *rotation* for aligning two multi-object complexes together.

The correspondence between SPHARM models is implied by the underlying parameterization: two points with the same parameter pair (θ, ϕ) on two surfaces are defined to be a corresponding pair. To register multi-object complexes, traditional methods [23, 24] rotate the parameter net of each individual model to a canonical position on its FOE for establishing the surface correspondence (Fig. 3), and then use the rigid-body Procrustes method to align reconstructed

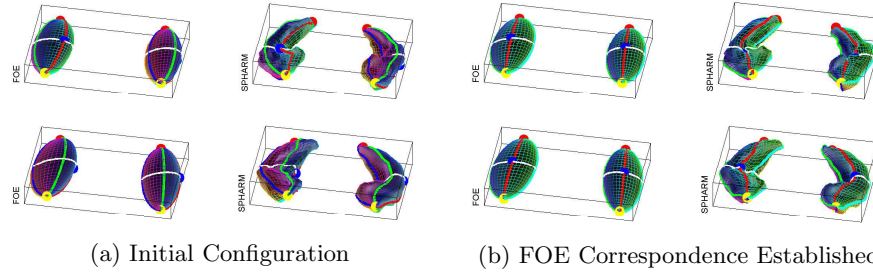


Fig. 3. Using first order ellipsoids (FOEs) to establish surface correspondence between two subjects: Each row corresponds to one subject, where both FOEs and the Degree 15 SPHARM reconstructions are displayed. The underlying parameterization defines the correspondence between SPHARM models and is shown as a colorful mesh superimposed onto the surface. Shown in (a) is the initial configuration of each subject, where the parameter nets are not aligned well. Shown in (b) is the result of rotating the FOEs to a canonical position to establish surface correspondence across subjects.

surface samples. These methods work well only if the FOE is a real ellipsoid (e.g., hippocampal case) but not an ellipsoid of revolution or a sphere. To remove this restriction, we developed a registration method by minimizing the root mean squared distance (RMSD) between two SPHARM models instead of aligning the FOEs [22]. Here, we extend this work to handle multi-object complexes.

Our approach shares a similar idea with the iterative closest point (ICP) method [25]. We start with an initial alignment and alternately run the following two steps to refine the alignment until it converges: (1) object space registration for aligning corresponding surface parts, and (2) parameter space registration for refining the surface correspondence. Suppose that we want to register a multi-object complex X to an atlas A . To create an initial alignment, we can first align X to A in the object space and then rotate the parameter net of each SPHARM model in X to best match its counterpart in A . In hippocampal cases, the initial alignment can be established by applying the FOE method. In cases where the FOE method does not apply, we can use ICP for initial alignment (see [22]).

In object space registration, we aim to improve the alignment in the object space. Since an initial surface correspondence has already been created, we can simply create corresponding surface samples between X and A and then align two corresponding point sets together in a least squares sense [25]. For convenience, we call this method as CPS (*i.e.*, aligning corresponding point sets). Let \mathbf{T} be the vector that translates the X center to the A center, and \mathbf{R} be the rotation matrix returned by CPS. We use the following approach to apply \mathbf{T} and \mathbf{R} to each SPHARM model in X and derive a new SPHARM representation that matches A . Let $\mathbf{v}(\theta, \phi) = \sum_{l=0}^{\infty} \sum_{m=-l}^l \mathbf{c}_l^m Y_l^m(\theta, \phi)$ be a SPHARM model. After applying translation \mathbf{T} and rotation \mathbf{R} , the new coefficients $\mathbf{c}_l^m(\mathbf{T}, \mathbf{R})$ can be calculated as follows: (1) $\mathbf{c}_0^0(\mathbf{T}, \mathbf{R}) = \mathbf{c}_0^0 + \mathbf{T} \times 2\sqrt{\pi}$, and $\mathbf{c}_l^m(\mathbf{T}, \mathbf{R}) = \mathbf{R} \times \mathbf{c}_l^m$ for $l, m > 0$.

In parameter space registration, we aim to improve the surface correspondence between SPHARM models that are roughly aligned in the object space.

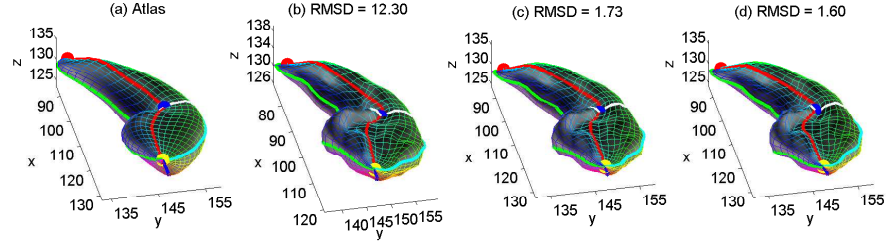


Fig. 4. Sample registration procedure: (a) The atlas. (b) The initial configuration of an individual, where the surface correspondence to the atlas has been established by FOE. (c) Result of object space registration. (d) Result of parameter space registration. RMSD (in mm) is shown. The parameter net is shown as a colorful mesh on the surface.

Since the underlying parameterization defines the correspondence between different SPHARM surfaces, our task is to rotate the parameterization of one model to best match the other's. The goodness of the match is measured by the root mean squared distance (RMSD) between two models. RMSD can be calculated directly from SPHARM coefficients. Let S_1 and S_2 be two SPHARM surfaces, where their SPHARM coefficients are formed by $\mathbf{c}_{1,l}^m$ and $\mathbf{c}_{2,l}^m$, respectively, for $0 \leq l \leq L_{max}$ and $-l \leq m \leq l$. The RMSD between S_1 and S_2 can be calculated as:
$$\text{RMSD} = \sqrt{\frac{1}{4\pi} \sum_{l=0}^{L_{max}} \sum_{m=-l}^l \|\mathbf{c}_{1,l}^m - \mathbf{c}_{2,l}^m\|^2}$$
. We employ a sampling-based strategy that fixes one parameterization and rotates the other to optimize the surface correspondence by minimizing the RMSD. The rotation space can be sampled nearly uniformly using icosahedron subdivisions [22]. A naive solution for rotating the parameterization of a SPHARM model is to recalculate the coefficients using the rotated parameterization. However, it requires solving 3 linear systems and is time-consuming. To accelerate the process, we use a rotational property in the harmonic theory and rotate SPHARM coefficients without recalculating the expansion. Details about this method is available in [22].

While traditional registration methods [23, 24] derive sampled point distribution models as results, our algorithm operates directly on the SPHARM coefficients and so the results are still SPHARM models. This leads to a better potential of enhancing the registration results in addition to having a capability of performing subsequent analyses in both spatial and frequency domains. Fig. 4 shows a sample registration procedure, and we can see that our algorithm can further improve the FOE registration result with a reduced RMSD.

4 Results of Comparing MT and FS Data

We compared hippocampal volume between the MT and FS data in [19] and they showed good agreement (ICCs $\in [0.8, 0.85]$). In this work, we aim to examine additional morphometric features. Thus, we first exclude volume from all the MT and FS data: Each hippocampal pair is scaled proportionally along with the

corresponding ICV so that the ICV is normalized to 1421.2 cm^3 (i.e., the mean ICV of the MT data). The subsequent analyses are performed on the data after this scaling normalization.

4.1 Atlas Generation and Data Registration

We first use all the healthy controls ($n = 39$) in the MT data to create an atlas that represents an average normal hippocampal pair. Our method is as follows: (1) let the atlas be the first hippocampal pair; (2) register each pair to the atlas; (3) let the atlas be the mean of all the data; (4) repeat (2) and (3) until the atlas converges. The resulting atlas is shown in the first panel of Fig. 5(a).

Our overall strategy for aligning the MT and FS data together is as follows: (1) register all the MT data to the atlas; and (2) register each hippocampal pair in the FS data to its counterpart in the MT data. We consider two types of registration: a global one and a local one [23]. In *global registration*, we directly apply the algorithm proposed in Section 3 for aligning multi-object complexes. This rigid-body algorithm excludes only global translation and rotation and so the spatial relation between the two hippocampi or the pose of the hippocampal pair is preserved. In *local registration*, each individual hippocampus is allowed to match its template separately. This method expects to derive a better RMSD by allowing local translation and rotation and may account for possible non-rigid-body transformation effects introduced by the FS method.

We use RMSD to measure the registration error between an individual and its template. Fig. 5 shows sample global and local registration results for the MT and FS hippocampal traces of a same subject. While both methods can derive good registration results, the local method does generate better RMSDs. The following table shows a comparison of applying various registration methods on the MT and FS data, where each entry records (mean \pm std) of the registration errors for all subjects in a particular data set by a certain method.

	MT Data			FS Data		
	FOE-PRM	FOE-OBJ	OUR-ALG	FOE-PRM	FOE-OBJ	OUR-ALG
Global	16.12 ± 2.32	2.93 ± 0.73	2.84 ± 0.76	13.97 ± 3.52	3.32 ± 0.50	3.08 ± 0.50
Local	16.12 ± 2.32	1.88 ± 0.37	1.82 ± 0.34	14.03 ± 3.50	2.81 ± 0.42	2.76 ± 0.41

FOE-PRM: Rotate parameterization to a canonical position using FOEs.

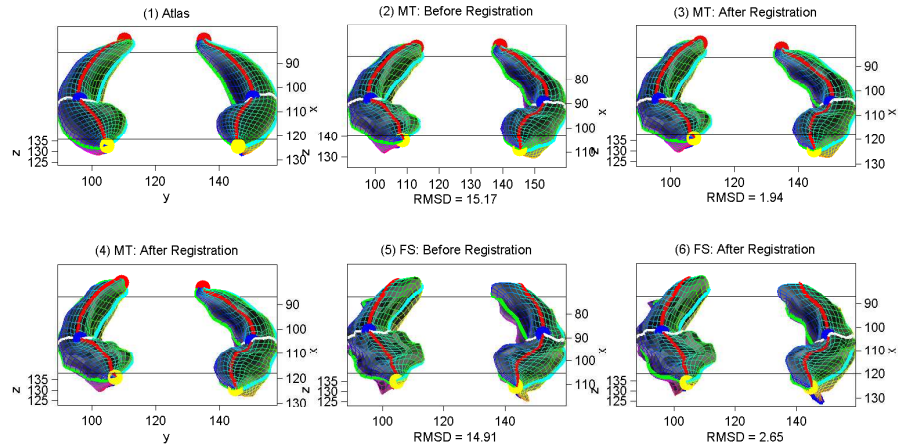
FOE-OBJ: One run of object space registration after FOE-PRM.

OUR-ALG: Our algorithm. Global: Global registration. Local: Local registration.

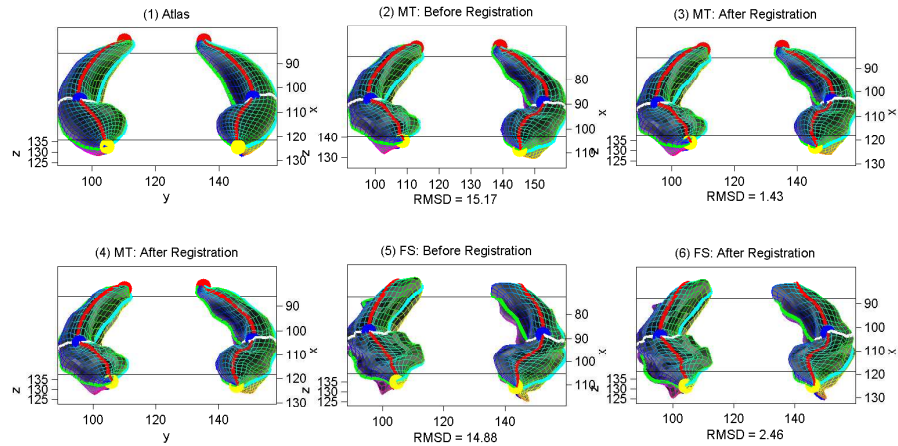
Although the traditional SPHARM registration methods work well on hippocampal data (see the FOE-OBJ columns for their results), our algorithm is able to further improve these results (see the OUR-ALG columns).

4.2 Position, Orientation, and Shape

While global registration excludes global effects on translation and rotation, the spatial relationship between the two hippocampi is preserved. We use the globally registered FOE model to define this local pose information, including



(a) Global registration: The spatial relationship between two hippocampi is preserved during the registration procedure.



(b) Local registration: Each hippocampus is individually aligned to best fit its template. The spatial relationship between two hippocampi is not preserved.

Fig. 5. Global registration (a) and local registration (b) for a same subject. In each of (a) and (b): Shown in the first row are (1) the atlas to which the MT model is registered, (2) the initial MT model, and (3) the registered MT model; and shown in the second row are (4) the MT model to which the FS model is registered (i.e., the same as (3)), (5) the initial FS model, and (6) the registered FS model. RMSDs are shown. The underlying parameterization is shown as a colorful mesh on each surface.

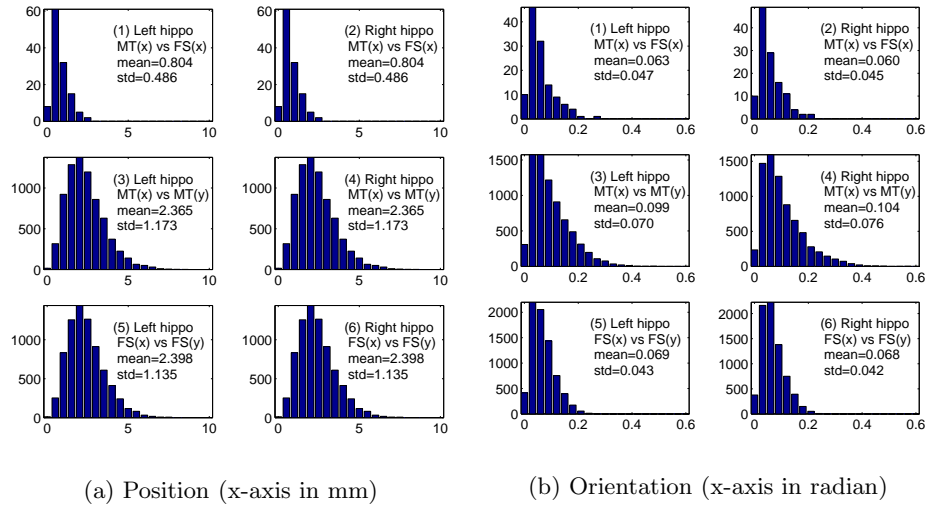


Fig. 6. Distributions of intra-subject and inter-subject distances on (a) position measures and (b) orientation measures after global registration. In each of (a) and (b), the left column shows the results for the left hippocampi and the right column for the right ones. Shown in the top row is intra-subject distances between the MT and FS methods, in the middle row inter-subject distances within the MT data, and in the bottom row inter-subject distances within the FS data.

the position and orientation of each hippocampus. Let h be a hippocampus, SP_h be its SPHARM model that is registered in the atlas space, P_h be the FOE center of SP_h , and N_h be the FOE north pole of SP_h (see Fig. 3 for sample FOEs on which north poles are shown as yellow dots). We define P_h to be the position measure of h and $O_h = \frac{N_h - P_h}{|N_h - P_h|}$ to be the orientation measure of h .

We report our work in progress on comparing the position and orientation measures determined by the MT and FS methods. We use the position measure of the left hippocampus as an example to show our approach. Let S be our subject set. Given a subject $x \in S$, we use l_x^M to denote its left hippocampus determined by the M method, where $M \in \{MT, FS\}$. We start with a simple examination of three sets of position distances: (1) intra-subject distances between the MT and FS methods: $D_{mtfs} = \{|P_{l_x^{MT}} - P_{l_x^{FS}}| \mid x \in S\}$; (2) inter-subject distances within the MT data: $D_{mtmt} = \{|P_{l_x^{MT}} - P_{l_y^{MT}}| \mid x, y \in S, x \neq y\}$; and (3) inter-subject distances within the FS data: $D_{fsfs} = \{|P_{l_x^{FS}} - P_{l_y^{FS}}| \mid x, y \in S, x \neq y\}$. Similar calculations are applied to the right hippocampus and the orientation measures. The orientation distance is measured by the angle between two directions.

Fig. 6 shows the distributions of all these distance collections. The MT and FS methods show good agreement on position measures: The intra-subject distances between the two methods (D_{mtfs}) are narrowly distributed and close to zeros, compared with large inter-subject variations shown in both MT data

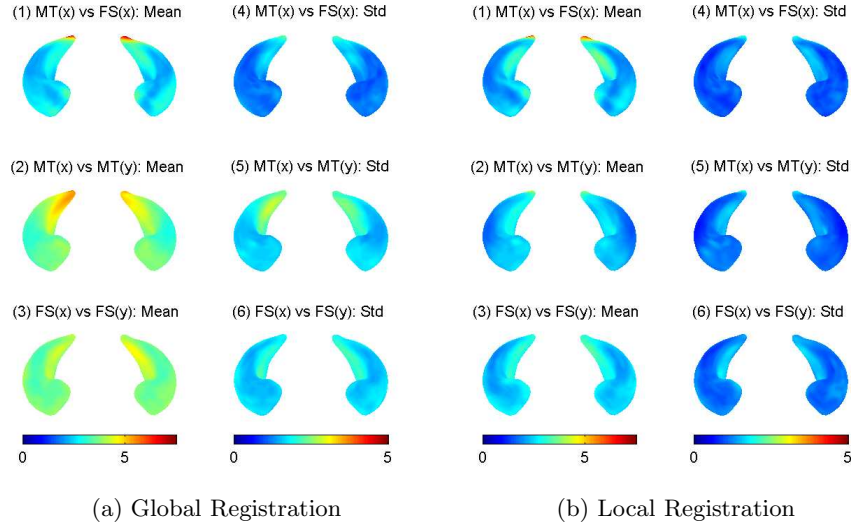


Fig. 7. Statistical maps of intra-subject and inter-subject surface distances after (a) global registration or (b) local registration. In each of (a) and (b), the left column shows the mean map, and the right column shows the standard deviation map. Shown in the top row is intra-subject distances between the MT and FS methods, in the middle row inter-subject distances within the MT data, and in the bottom row inter-subject distances within the FS data. All the mean and standard deviation maps are color-coded and superimposed onto the hippocampal atlas.

(D_{mtmt}) and FS data (D_{fsfs}). As to orientation, the intra-subject distances between the two methods are similar to the inter-subject distances within either of the methods. All these distances are small, suggesting a consistent similarity in relative orientations between two hippocampi. For local registration, we did the same experiments, and all the distances on position or orientation measures became zero. This indicates that local registration excludes not only global but also local translation and rotation effects of each individual hippocampus.

Finally we examine the shape measures. Since we have established surface correspondence among SPHARM models, given any two models, we can calculate a distance map showing the model difference on each surface location. Similar to the position and orientation cases, we calculate three sets of distance maps: (1) intra-subject distances between MT and FS methods, (2) inter-subject distances within the MT data, and (3) inter-subject distances within the FS data. Since it is hard to visualize the distance distribution for all the surface locations, we only show the mean and standard deviation of these distance maps in Fig. 7.

For global registration, compared with the inter-subject distances within a method (MT or FS), the intra-subject distances between two methods are relatively small. This indicates some degree of agreement, but it might be related only to position and orientation factors, since globally registered models contain not only shape but also position and orientation information. In local reg-

istration, the position and orientation information is excluded, and the intra-subject distances between the methods and the inter-subject distances within the method become at a similar level. To make the two methods agree more on the hippocampal shape, it appears there is still room for improvement. In particular, the tail region shows a notable systematic difference. By a visual inspection of the raw data (see Fig. 1 for example), we notice that the FS results tend to have a fatter tail and some noisy spikes on the surface.

5 Conclusions

We have compared an automated method, FreeSurfer (V4), with a published manual protocol on the determination of hippocampal boundaries from MRI scans, using data from an existing MCI/AD cohort. This comparison is enabled by an improved SPHARM modeling and registration procedure designed for a multi-object setting. We use a global registration process to extract relative position and orientation measures of the two hippocampi, and the manual and FreeSurfer methods show good agreement on these measures. We use a local registration process to account for possible non-rigid-body effects introduced by FreeSurfer and extract fine-scale surface shape measures, and the two methods show less agreement on these measures. Visual inspection of raw data shows the FreeSurfer results tend to have a fatter tail and some noisy spikes on the surface. Work is in progress to examine a refined FreeSurfer segmentation strategy and an improved agreement on shape features is expected. Other interesting future topics include: (1) Can the results be greatly improved by involving minimal human intervention? (2) Is there any systematic difference between the criteria used by the two methods? (3) Are the discriminative powers to detect disease similar between the manual and FreeSurfer data? (4) Test other statistics such as intra-class correlation coefficients to cross-validate the inter-rater reliability.

Acknowledgements: Supported in part by NIBIB/NEI R03 EB008674-01, NIA R01 AG19771, NCI R01 CA101318 and U54 EB005149 from the NIH, Foundation for the NIH, and grant #87884 from the Indiana Economic Development Corporation (IEDC). We thank Nick Schmansky and Bruce Fischl of Harvard Medical School and Randy Heiland of Indiana University for help with running FreeSurfer on IU's supercomputers.

References

1. Thompson, P., Hayashi, K., et al.: Mapping hippocampal and ventricular change in alzheimer disease. *Neuroimage* **22** (2004) 1754–66
2. Saykin, A.J., Wishart, H.A., et al.: Older adults with cognitive complaints show brain atrophy similar to that of amnesic MCI. *Neurology* **67** (2006) 834–842
3. Wang, L., Beg, F., Ratnanather, T., et al.: Large deformation diffeomorphism and momentum based hippocampal shape discrimination in dementia of the alzheimer type. *IEEE Trans Med Imaging* **26** (2007) 462–70

4. Csernansky, J., Wang, L., Swank, J., Miller, J., Gado, M., McKeel, D., Miller, M., Morris, J.: Preclinical detection of alzheimer's disease: hippocampal shape and volume predict dementia onset in the elderly. *Neuroimage* **25** (2005) 783–92
5. Hogan, R., Wang, L., Bertrand, M., et al.: Predictive value of hippocampal mr imaging-based high-dimensional mapping in mesial temporal epilepsy: preliminary findings. *AJNR Am J Neuroradiol.* **27** (2006) 2149–54
6. Csernansky, J., Wang, L., et al.: Hippocampal deformities in schizophrenia characterized by high dimensional brain mapping. *Am J Psychiatry* **159** (2002) 2000–6
7. Gerig, G., Styner, M.: Shape versus size: Improved understanding of the morphology of brain structures. In: MICCAI'2001, LNCS 2208. (2001) 24–32
8. Shenton, M., Gerig, G., McCarley, R., Szekely, G., Kikinis, R.: Amygdala-hippocampal shape differences in schizophrenia: The application of 3d shape models to volumetric mr data. *Psychiatry Res* **115** (2002) 15–35
9. Shen, D., Moffat, S., et al.: Measuring size and shape of the hippocampus in mr images using a deformable shape model. *Neuroimage* **15** (2002) 422–34
10. McHugh, T., Saykin, A., et al.: Hippocampal volume and shape analysis in an older adult population. *Clin Neuropsychol.* **21** (2007) 130–45
11. Yushkevich, P., Detre, J., et al.: Hippocampus-specific fmri group activation analysis using the continuous medial representation. *Neuroimage* **35** (2007) 1516–30
12. Iowa MHCRC Image Processing Lab: The Brains Software. <http://www.psychiatry.uiowa.edu/mhrc/IPLpages/BRAINS.htm>
13. NAMIC: 3D Slicer. <http://www.slicer.org/>
14. Yushkevich, P., Piven, J., Hazlett, H., Smith, R., Ho, S., Gee, J., Gerig, G.: User-guided 3d active contour segmentation of anatomical structures: significantly improved efficiency and reliability. *Neuroimage* **31** (2006) 1116–28
15. Mueller, S., Weiner, M., et al.: The alzheimer's disease neuroimaging initiative. *Neuroimaging Clin N Am.* **15** (2005) 869–77
16. Fischl, B., Sereno, M., AM, D.: Cortical surface-based analysis. ii: Inflation, flattening, and a surface-based coordinate system. *Neuroimage* **9** (1999) 195–207
17. Dale, A., Fischl, B., Sereno, M.: Cortical surface-based analysis. i. segmentation and surface reconstruction. *Neuroimage* **9** (1999) 179–94
18. Fischl, B., Salat, D., et al.: Whole brain segmentation: automated labeling of neuroanatomical structures in the human brain. *Neuron* **33** (2002) 341–55
19. Shen, L., Saykin, A.J., Firpi, H.A., West, J.D., et al.: Comparison of manual and automated determination of hippocampal volumes in MCI and older adults with cognitive complaints. *Alzheimer's & Dementia* **4**(4, suppl 2) (2008) T29–30
20. Tae, W., Kim, S., et al.: Validation of hippocampal volumes measured using a manual method and two automated methods (freesurfer and ibaspm) in chronic major depressive disorder. *Neuroradiology* (2008) Apr 15. [Epub ahead of print]
21. Brechbühler, C., Gerig, G., Kubler, O.: Parametrization of closed surfaces for 3D shape description. *Computer Vision & Image Understanding* **61**(2) (1995) 154–170
22. Shen, L., Huang, H., Makdeon, F., Saykin, A.J.: Efficient registration of 3D spharm surfaces. In: 4th Canadian Conf. on Computer & Robot Vision. (2007) 81–88
23. Styner, M., Goczowski, K., et al.: Statistics of pose and shape in multi-object complexes using principal geodesic analysis. *LNCS* **4091** (2006) 1–8
24. Shen, L., et al.: Shape-based discriminative analysis of combined bilateral hippocampi using multiple object alignment. In: SPIE Proc. 5370 (2004) 274–282
25. Besl, P.J., McKay, N.D.: A method for registration of 3-D shapes. *IEEE Trans. on PAMI* **14**(2) (1992) 239–256